UNLIMITED
UNCLASSIFIED

ILLIMITÉ
NON CLASSIFIÉ

Technical Report

Rapport technique

1988 / 01

TR-TM-006
NRC NO. 28862

# IMPACT AND FRETTING WEAR STUDIES
# PART 2 — ROOM TEMPERATURE TEST RESULTS
# (SINGLE IMPACT per CYCLE)

P.L. Ko, L. Close and M.F. Robertson

Division of
Mechanical Engineering

Division de
génie mécanique

National Research Council Canada
Conseil national de recherches Canada

Canada

89-02357/

## DIVISION OF MECHANICAL ENGINEERING PUBLICATIONS

**DM** **(Division of Mechanical Engineering Report)**
Scientific and technical information considered important, complete and a lasting contribution to existing knowledge.

**TR** **(Technical Report)**
Information less broad in scope but a substantial contribution to existing knowledge.

**CTR** **(Controlled/Classified Technical Report)**
A Technical Report with controlled distribution for national security, proprietary or other reasons.

**LM** **(Laboratory Memorandum)**
Preliminary or exploratory information with controlled distribution.

**CAT** **(Calibration Analysis and Test Report)**
Information on minor laboratory projects or services.

## PUBLICATIONS DE LA DIVISION DE GÉNIE MÉCANIQUE

**DM** **(Rapport de la Division de génie mécanique)**
Informations scientifiques et techniques jugées importantes, complètes et susceptibles de contribuer de façon durable à l'avancement des connaissances courantes.

**TR** **(Rapport technique)**
Informations de moindre importance, mais pouvant contribuer substantiellement à l'avancement des connaissances actuelles.

**CTR** **(Rapport technique à diffusion contrôlée/classifiée)**
Rapport technique à diffusion contrôlée pour des raisons de sécurité nationale, de propriété intellectuelle et autres.

**LM** **(Mémoire de laboratoire)**
Informations préliminaires ou de nature exploratoire à diffusion contrôlée.

**CAT** **(Rapport d'étalonnage d'analyse et d'essai)**
Informations sur de petits projets ou des services de laboratoire.

UNLIMITED
UNCLASSIFIED

ILLIMITÉ
NON CLASSIFIÉ

# IMPACT AND FRETTING WEAR STUDIES

## PART 2 - ROOM TEMPERATURE TEST RESULTS (SINGLE IMPACT per CYCLE)

# ETUDES DE L'USURE PAR IMPACT ET DE L'USURE DE CONTACT

## PARTIE 2 - RÉSULTATS D'ESSAIS À TEMPÉRATURE AMBIANTE (UN IMPACT par CYCLE)

P.L. Ko, L. CLOSE and M.F. Robertson

Technical Report

1988/01

Rapport technique

TR-TM-006
NRC NO.28862

C. Dayson, Head/Chef
Tribology & Mechanics Laboratory/
Laboratoire de tribologie et de mècanique

J. Ploeg
Director/
directeur

**ACKNOWLEDGEMENT**

The authors would like to acknowledge the contributions of Mr. T. Vanderhoek, who designed the high temperature impact-fretting test rig, and Messrs. E. Bray and M. Simunek who manufactured and installed the test rig.

## ABSTRACT

Wear due to impacting and reciprocating sliding motion is studied in the new impact-fretting test rig. Two material combinations, namely steel vs steel and steel vs brass, have been tested with a single impact per cycle. The results show that adhesive wear and fatigue are the principal mechanisms in impact and reciprocating sliding wear, and that wear rate increases proportionally to the impact energy. However, the results also show a transition beyond which mild wear becomes severe.



## RÉSUMÉ

On étudie l'usure créée par impact et par glissement alternatif dans le nouvel appareillage d'essai de l'usure par impact et frottement. Les deux combinaisons des matériaux, acier contre acier et acier contre laiton, ont été soumis à des essais à un seul impact par cycle. Les résultats indiquent que l'usure par adhésion et fatigue sont les principaux mécanismes de l'usure par impact et glissement alternatif, et que le taux de vitesse d'usure augmente proportionnellement à l'énergie de l'impact. Cependant, ils indiquent également qu'il existe une zone de transition au-delà de laquelle l'usure légère devient importante.

CONTENTS


| | | Page |
|---|---|---|
| | ACKNOWLEDGEMENTS | (ii) |
| | ABSTRACT/RÉSUMÉ | (iii) |
| | LIST OF ILLUSTRATIONS | (v) |
| | LIST OF TABLES | (v) |
| 1.0 | INTRODUCTION | 1 |
| 2.0 | EXPERIMENTAL SETUP | 2 |
| 3.0 | TEST METHOD | 3 |
| 4.0 | TEST RESULTS | 3 |
| | 4.1 Steel vs Steel Tests | 4 |
| | 4.1.1 Impact energy | 4 |
| | 4.1.2 Impact cycles | 4 |
| | 4.1.3 Surface Finish | 4 |
| | 4.2 Steel vs Brass Tests | 4 |
| | 4.2.1 Impact energy | 4 |
| | 4.2.2 Impact cycles | 4 |
| 5.0 | ANALYSIS OF RESULTS AND DISCUSSION | 4 |
| | 5.1 Wear Rate | 5 |
| | 5.2 Wear Debris | 6 |
| | 5.3 Wear Scar | 6 |
| | 5.4 Transition | 6 |
| 6.0 | PROPOSED IMPACT WEAR MODEL | 7 |
| 7.0 | CONCLUSIONS | 7 |
| 8.0 | REFERENCES | 8 |
| | DOCUMENTATION PAGE | |

## LIST OF ILLUSTRATIONS


| Figure | | Page |
|---|---|---|
| 1 | General layout of impact-fretting test rig | 9 |
| 2 | Specimen-exciter connection | 10 |
| 3 | Close-up view of the specimen assembly | 11 |
| 4 | Time based impact force and sliding displacement traces | 12 |
| 5 | Impact force vs sliding displacement | 13 |
| 6 | Wear rate vs impact energy (steel vs steel) | 14 |
| 7 | Mass loss vs number of impact cycle (steel vs steel) | 15 |
| 8 | Wear rate vs impact energy (steel vs brass) | 16 |
| 9 | Mass loss vs number of impact cycle (steel vs brass) | 17 |
| 10 | Linearized wear rate vs impact energy (steel vs steel) | 18 |
| 11 | Photomicrographs of steel wear particles | 19 |
| 12 | Photomicrographs of brass wear particles | 20 |
| 13 | Photographs of wear scars (steel) | 21 |
| 14 | Photomicrographs of wear scars (steel and brass) | 22 |
| 15 | Microsurface profile traces of the worn areas | 23 |
| 16 | Burwell's asperity contact models | 24 |


## LIST OF TABLES


| Table | | Page |
|---|---|---|
| 1 | (A) Mechanical and physical properties and (B) Ranges and limits of specimens | 25 |
| 2 | Test results and some input parameters of steel vs steel | 26 |
| 3 | Test results and some input parameters of steel vs brass | 27 |

# IMPACT AND FRETTING WEAR STUDIES
# PART 2 - ROOM TEMPERATURE TEST RESULTS (SINGLE IMPACT per CYCLE)

## 1.0 INTRODUCTION

Wear is defined as the progressive loss of substance from the operating surface of a body, occurring as a result of relative motion at the surface. Mechanical action on the surface of materials may be sliding, rolling, spinning, impact, oscillation, and flow. In many mechanical components some form of vibration is unavoidable, and fretting wear arises when contacting surfaces undergo oscillatory tangential displacement of small amplitude (Waterhouse 1972). In situations where a clearance exists, wear may be also a result of both impacting and reciprocating rubbing.

Fretting wear, impact wear, and wear due to a combination of impacting and reciprocating rubbing may be found in small components and large components. For examples, wear has been found in electrical contacts and types and ribbons of printing equipment, as well as on sucker rods and tubes in deviated oil wells and swivel connections in offshore drilling equipment. There are severe wear damages due to impact and sliding in mining and forging operations and in the wear of wire ropes, gear teeth, and claws on pinions and couplings. Impact fretting wear is also a common tribology problem in a wide range of power plant machinery, such as in steam generators, heat exchangers, and reactor fuel rods and control rods. The continuous demands for increased efficiency of these components have inevitably led to higher stresses and vibration levels, often resulting in higher wear rates.

Understanding the mechanics and various mechanisms involved in these wear situations helps in the assessment of the useful life of impacting and sliding components in practical situations. Although there exist many wear design handbooks and wear equations, many of these apply only to situations of either pure sliding or impacting. It is only very recently that attempts have been made to understand and develop models for wear problems subjected to "compound impact" or combined impacting and reciprocating sliding situations.

Under compound impact mode, the shear stress becomes an important factor affecting wear damage (Rice et al. 1980; Ko 1985). Engel (1976) and his colleagues showed that the contribution of the normal component is small compared with that of the sliding component and that the larger the sliding speed component, the sooner wear is initiated. Rice et al. (1980) also found that the relative transverse sliding velocity and the peak normal impulsive stress are significant parameters on the wear of titanium alloys under repetitive compound impact.

Rabinowicz and Hozaki (1985) studied impact wear of ductile metals. They concluded that impact wear is not itself a form of wear but

merely describes one way in which the normal force and shearing action required to produce friction and wear can be applied. Depending on the circumstances, any type of wear could account for the major proportion of the material removed. Since adhesive wear is the most important form of wear in ordinary sliding, it is, therefore, also very prominent during impact conditions. Ko et al. (1982) arrived at a similar conclusion in their studies of heat exchanger tube fretting wear.

Ko et al. (1984) and Ko (1985) showed that tube fretting wear was related to the dynamic interaction (impact force) between the tube and its support. He statistically analyzed the resultant impact forces for different types of tube motion to obtain a force function. This was later correlated with the wear rate. The approach, however, did not differentiate the significance of the shear and normal components on wear. Arbitrary weighting coefficients had to be used. In a later approach (Ko 1985), the x-y displacement signals of the tube motion were recorded simultaneously with the force signals. The force signals were resolved into normal and tangential components based on the instantaneous tube trajectory during tube/support contact. The wear rate correlated well with the force function derived from the tangential force component.

Levy and Morri (1985) treated impact wear as an elastic-contact dominated process, with load and relative slip during contact as the most crucial governing parameters. The load-sliding distance integral was considered to be directly dependent on the incident kinetic energy.

A research program to develop an impact-fretting wear predictive model using the impact energy as the principal parameter has been initiated. The present report represents the second interim report for this program. It describes the results of a series of oblique impact tests obtained from the new impact-fretting test rig (Ko 1987) at room temperature.

## 2.0 EXPERIMENTAL SETUP

Figure 1 shows a general layout of the test rig. It consists of two 300 N electro-magnetic shakers and two specimens housed inside an autoclave. These shakers can either drive one specimen together or both specimens individually. In the present arrangement both shakers, mounted at 90° to each other, are connected to the dynamic specimen. A phase-lock frequency generator controls the shakers and provides impact motion between the dynamic and stationary specimens at any desired angle, including pure normal impact and pure reciprocating sliding.

The bullet shaped dynamic specimen is mounted on a ring shaped specimen holder. Two flexible push rods link the holder to the shakers by way of flexures and bellows [Fig. 2]. A triaxial force transducer holds the stationary flat specimen and is attached to a semicircular bar with its ends fixed on to the middle section of the autoclave. The specimen section of the bar passes through the central opening of the dynamic specimen holder [Fig. 3].

The autoclave is designed to operate in air or other gaseous environments at temperatures up to 300°C. It can also be operated in fluid environments at temperatures up to 100°C.

The shakers have a frequency range from dc to 7500 Hz. A maximum displacement of 9.5 mm is obtainable at frequencies up to 32 Hz. They deliver a peak force of 311 N or 200 Nrms.

## 3.0 TEST METHOD

The shaker that controls motion in the normal direction also provides the static normal force by exerting a biased dc voltage to the moving coil. For higher static normal forces, a mechanical loading device is used.

In the present series of tests the hammer (dynamic specimen) would impact the target (stationary specimen) at a 45° angle once during each cycle. The hammer would slide a certain distance across the target due to the oblique nature of the impact, and then bounce off the target due to elastic recoil. A proximity transducer mounted on the crossbar that held the stationary specimen monitors the relative movement between the two specimens.

The stationary specimen is a disc 25 mm in diameter and 3 mm thick. It is mounted on a triaxial force transducer that monitors the normal and the tangential forces. Figure 4 shows a typical digitized oscilloscope trace of the time-based sliding displacement and impact force in the major tangential direction. Figure 5 shows a force vs displacement curve reproduced from the two curves in Figure 4. The area under the curve provides a measure of the impact energy (work done on the target) during each impact. All the conversions and calculations are done in a computer using the stored data from the oscilloscope.

Mass loss due to wear was found by weighing the stationary specimen before the test and after a number of impact cycles. The mass loss from the hardened dynamic specimen was insignificant.

All of the tests were conducted in air at room temperature. With the exception of the first set of tests, all had a jet of air (0.2 MPa) directed over the impact area to keep the contact surface free of wear debris.

## 4.0 TEST RESULTS

The parameters tested include energy levels, cycle numbers, ratios of shaker inputs, and two material combinations. In the first series of tests, the dynamic and stationary specimens are respectively a hardened carbon steel (4340, RC 55-60) hammer and carbon steel (12L14) blanks. In the second series of tests, the specimens are a hardened carbon steel hammer and free cutting yellow brass (C36000) blanks.

Table 1 gives some of the mechanical and physical properties and dimensions of the specimens. Tables 2 and 3 show the weight loss results of all tests, including the input and output parameters from the first and the second series of tests.

### 4.1 Steel vs Steel Tests

#### 4.1.1 Impact energy

In Figure 6 the weight loss of the stationary specimen after 54000 cycles was plotted against the impact energy calculated from the impact force and the relative sliding distance between the two specimens. Curve A is from tests with a jet of air blowing over the impact area of the surfaces and curve B is from tests performed without the jet of air. They show that wear rate increases exponentially with impact energy in both cases and is higher when the surfaces are free of wear debris.

#### 4.1.2 Impact cycles

Figure 7 shows the change in weight loss with the number of impacts for six impact energy levels. At low impact energy levels, the weight loss appears to increase linearly with impact cycle. At higher impact energy levels, two wear rates appear; the wear rate is higher initially and changes into a lower wear rate after a number of impact cycles.

#### 4.1.3 Surface finish

One set of tests was repeated using an impact hammer with a roughened surface. The results showed no measurable difference in wear rate.

### 4.2 Steel vs Brass Tests

#### 4.2.1 Impact energy

The wear rate of brass in the steel vs brass series is more than an order of magnitude higher than the wear rate of steel in the steel vs steel series. The results in Figure 8 also show that the wear rate of brass diverges when the impact energy exceeds 10 mJ/cycle. Beyond this point a second curve with a much steeper slope appears.

#### 4.2.2 Impact cycles

With brass specimens, the transition from high wear rate to low wear rate is not apparent, particularly at the higher impact energy level, as illustrated in Figure 9. The wear rates increase linearly with increasing number of impact cycles.

## 5.0 ANALYSIS OF RESULTS AND DISCUSSION

The wear equation for sliding wear, $V/L = k(F_n/3p_m)$, can be modified to fit an impact and reciprocating sliding wear model, thus

$$V/n = k_1(E_i/P_m) \qquad (1)$$

where $E_i$ = impact energy = $F_s d$

$F_s$ = impact force in the tangential direction

$d$ = relative slid distance per impact cycle

$V/n$ = volume of wear per cycle, $n$ = total number of cycles

$p_m$ = yield strength of the softer material (mean flow pressure or indentation hardness)

From the above equation, a graph of the wear rate vs the impact energy should yield a straight line with a slope equal to the wear coefficient $k_1$ divided by the yield strength $p_m$. However, the curves in Figure 7 suggest that the initial wear rate is much higher and not constant; it only becomes linear after a number of cycles. The transition depends on the impact energy; the higher the impact energy, the longer it takes to reach the transition point.

### 5.1 Wear Rates

The results in Figure 7 clearly show that for each impact energy tested there are two wear rates. In each case a higher wear rate initially is followed by a lower one. The transition appears to vary with the impact energy; the lower the impact energy, the sooner the transition occurs.

For wear of steel in air the combined effect of the initial wear rate and the rate of oxidation would influence the transition to the steady state (lower) wear rate. When the initial wear rate is low due to low impact energy, there is sufficient time for the contact surface to form a protective oxide film of adequate thickness very early on. At higher impact energy, the initial wear rate is higher and it takes longer time to build up an effective surface film. At even higher impact energy, the high initial wear rate persists and there is not sufficient time to form a protective film. Ko (1979) observed similar behaviour in the wear of zirconium alloys. These alloys are readily oxidized when exposed in air.

Brass does not form a protective surface film as readily as steel and zirconium alloys, and the wear of brass behaves differently. As illustrated in Figure 9, the wear loss increases linearly with increasing number of cycles.

Figure 10 shows a plot of impact energy vs wear rate for steel using the lower (steady state) wear rates from the curves in Figure 7. The results show that the relationship is linear for impact

energies above 20 mJ/cycle. Below this energy the wear rate becomes very low. Engel's zero impact wear model (Engel et al. 1973) estimates that, for steel vs steel, the zero wear life is more than one-half million cycles when the maximum Hertzian pressure is about one third of the uniaxial tensile yield strength of steel.

### 5.2 Wear Debris

It has been shown in fretting wear studies (Hurricks 1970; Ko 1979) that wear rate is often influenced by the ease with which wear debris is disposed. The wear debris of steel generated in reciprocating sliding wear are usually very fine and often acts as a protective coating when trapped between the contacting surfaces. Some of the wear particles that were collected and examined in a scanning electron microscope were about 0.005 sq.mm in size and oxidized [Fig.11]. Thus, if the wear debris are disposed of either by fluid flow as in steam generator tube/support or by a jet of air as in the present study, fresh materials are being continuously exposed and the wear rate would become higher. This is indeed the case, as illustrated in Figure 6.

In the case with brass, the wear debris varies in size from less than 0.01 sq.mm to slightly greater than 1 sq.mm and with a maximum thickness of about 0.05 mm. Their profiles resemble a flattened semi-ellipsoid with the flat surface on top which was deformed and flattened by the hardened steel hammer. The other side of the debris clearly shows that the direction of fracture follows the tangential motion. Indeed, the profile of these wear particles tends to resemble the Hertzian stress field [Fig. 12].

### 5.3 Wear Scar

With steel specimens, after the first few impacts, a small circular indentation was produced on the stationary specimen. With subsequent impacts, this crater steadily became wider and deeper. Figure 13 shows a series of photographs illustrating the progressive formation of the tear-shaped wear scar from the steel specimens.

Further examination of the worn area using both optical and scanning electron microscopes [Fig. 14a], revealed that adhesive wear was the principal mechanism for steel vs steel. This is in agreement with early findings by Ko (1982) and Rabinowicz and Hozaki (1985).

With brass specimens, there are two types of wear scar corresponding to the two divergent wear rate vs impact energy curves. The one with fine longitudinal scars corresponds to the curve with lower wear rates and regular hammer motion [Fig. 14b]. The other type of wear scar has a coarse appearance and corresponds to the curve with higher wear rates [Fig. 14c]. The former appears to be primarily due to adhesion and abrasion; the latter also shows evidence of fatigue and delamination. It was also observed during this latter type of tests that the hammer motion became erratic with periodic beating. This may result in more severe impacting loading and fatigue.

Figure 15 shows two microsurface profile traces of the dynamic (hammer) and stationary (anvil) specimens. The isometric presentation provides a perspective of the wear scar shape and size.

### 5.4 Transition

The results clearly show there is a transition beyond which mild wear becomes severe. Shaw (1968) attributed this to the interaction of the plastic zones beneath the contacting asperities. He used simple asperity contact diagrams to illustrate the two situations. During mild wear [Fig. 16a], there is no interaction between the plastic zones. As the impact force is increased, the plastic zones interact [Fig. 16b], and the subsurface regions become entirely plastic. This leads to massive cold welding and severe galling.

## 6.0 PROPOSED IMPACT WEAR MODEL

The experimental results show that wear, having reached the steady state, has a linear relationship with the impact energy and the number of impacts. However, for steel vs steel, a higher wear rate exists during the initial stage. A modified wear model to account for the transition is needed.

In developing this wear model, the oxidation rate of steel and the minimum oxide film thickness that becomes effective will have to be established first. This film is rubbed off continuously due to the wear process. Therefore, depending on the wear rate and the oxidation rate, an equilibrium could be reached after a number of cycles.

A model representing the transition from low wear rates to a linear higher wear rate also needs to include the material yield strengths and ratios of peak stress to yield stress, as used in the zero wear model. The formulation of this wear model will be published in the next report.

## 7.0 CONCLUSIONS

(1) Adhesion, fatigue, and delamination are the principal mechanisms in impact and reciprocating sliding wear.

(2) The wear rate of brass is more than an order of magnitude higher than the corresponding wear rate of carbon steel.

(3) For steel vs steel, wear increases linearly with number of cycles in two stages: a higher wear rate initially, followed by a constant lower wear rate.

(4) For steel vs brass, wear of the brass increases linearly with number of cycles throughout the test range.

(5) The wear rate of steel increases linearly with impact energy when the energy is above 20 mJ/cycle.

(6) The wear rate of brass increases with impact energy, but the rate of change increases significantly when the motion of the impact hammer becomes erratic.

## 8.0 REFERENCES

ENGEL, P.A., LYONS, T.H. and SIRICO, J.L., 1973.
Impact Wear Model for Steel Specimens. Wear 23: 185-201.

ENGEL, P.A., 1976. Impact Wear of Materials. Elsevier,The Netherlands.

HURRICKS, P.L., 1970. The Mechanism of Fretting - A Review.
Wear 15: 389-409.

KO, P.L., 1979. Wear of Zirconium Alloys due to Fretting and Periodic Impacting. Wear 55 (2): 369-384.

KO, P.L., TROMP, J.H. and WECKWERTH, M.K., 1982.
Heat Exchanger Tube Fretting Wear: Correlation of Tube Motion and Wear.
ASTM Special Technical Publication 780: 86-105.

KO, P.L. and BASISTA, H., 1984.
Correlation of Support Impact Force and Fretting Wear for a Heat Exchanger Tube. J. of Pressure Vessel Technology 106 (1): 69-77

KO, P.L., 1985.
The Significance of Shear and Normal Force Components on Tube Wear due to Fretting and Periodic Impacting. Wear 106 (1-3): 261-281.

KO, P.L., 1987.
Impact and Fretting Wear Studies, Part 1 - Test Rig and Review of Theories. National Research Council of Canada Report, NRC No.27948.

LEVY, G. and MORRI, J., 1985.
Impact Wear in CO2-based Environments. Wear 106: 97-138.

RABINOWICZ, E. and HOZAKI,K., 1985. Impact Wear of Ductile Metals.
Proc. of the JSLE International Tribology Conference, 2: 263-268.

RICE, S.L., NOWOTNY, H. AND WAYNE, S.F., 1980.
Formation of Subsurface Zones in Impact Wear.
ASLE preprint No. 80-AM-2D-3

RICE, S.L., WAYNE, S.F. and NOWOTNY, H., 1980.
Material Transport Phenomena in the Impact Wear of Titanium Alloys.
Wear 65 (2): 215-226.

SHAW, M.C., 1968.
Lubrication, Friction and Wear under Gross Plastic Deformation.
Friction and Wear Interdisciplinary Workshop, TM-X-52748.

WATERHOUSE, R.B., 1972. Fretting Corrosion. Pergamon Press Ltd, Oxford.

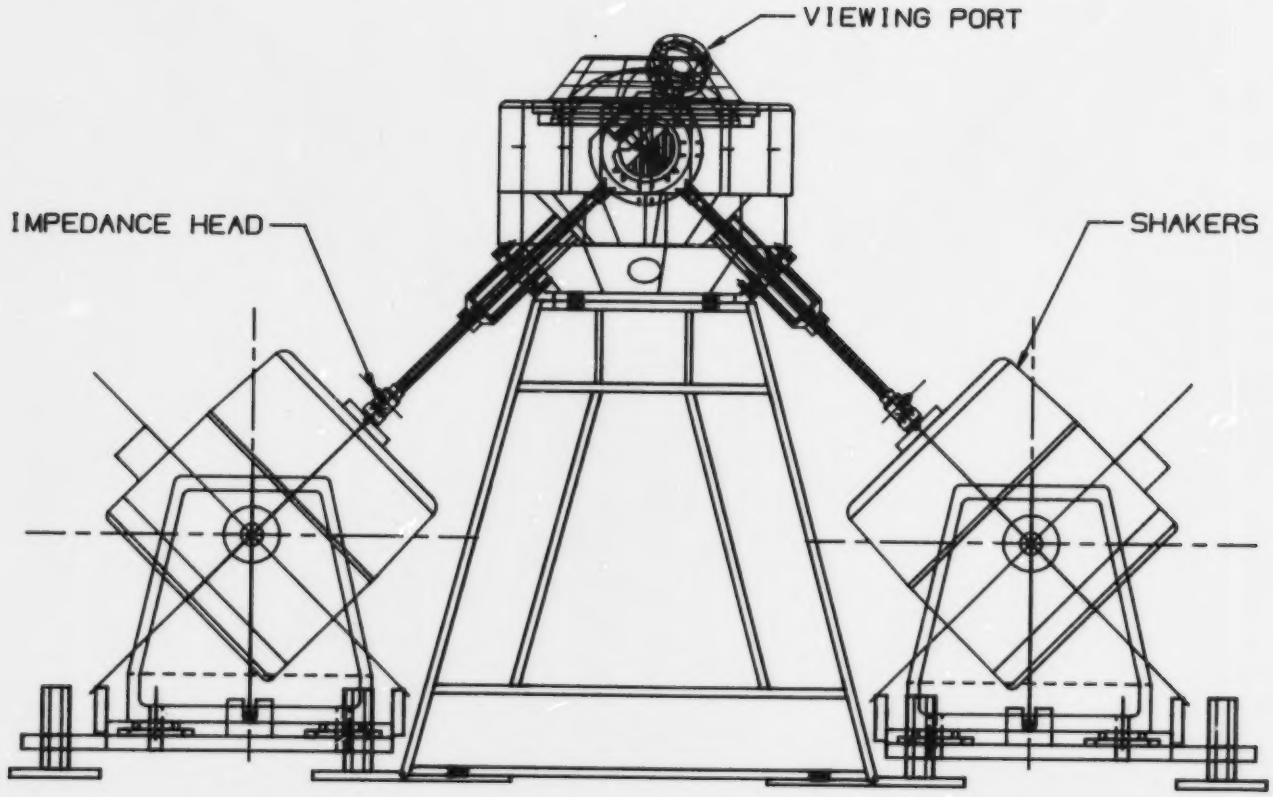


Fig. 1. General layout of impact-fretting test rig

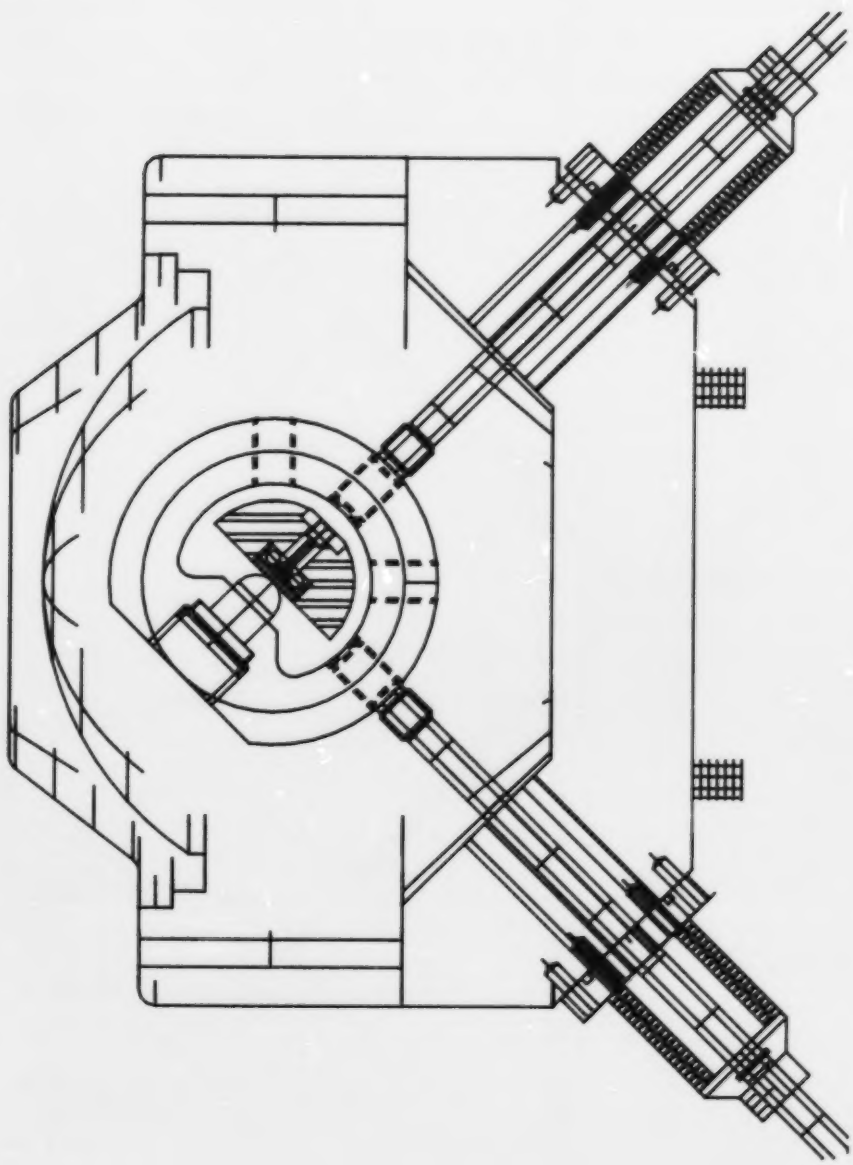

Fig. 2. Specimen-exciter connection

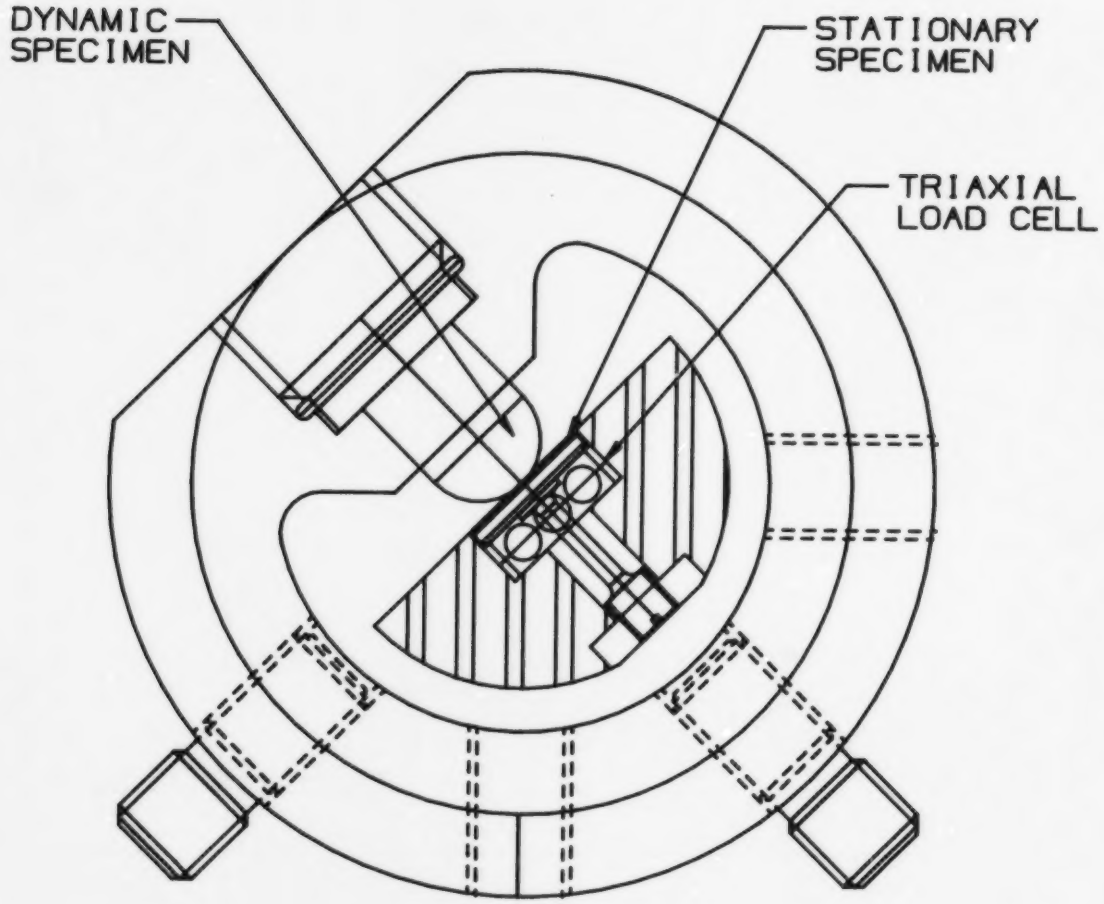


Fig. 3. Close-up view of the specimen assembly

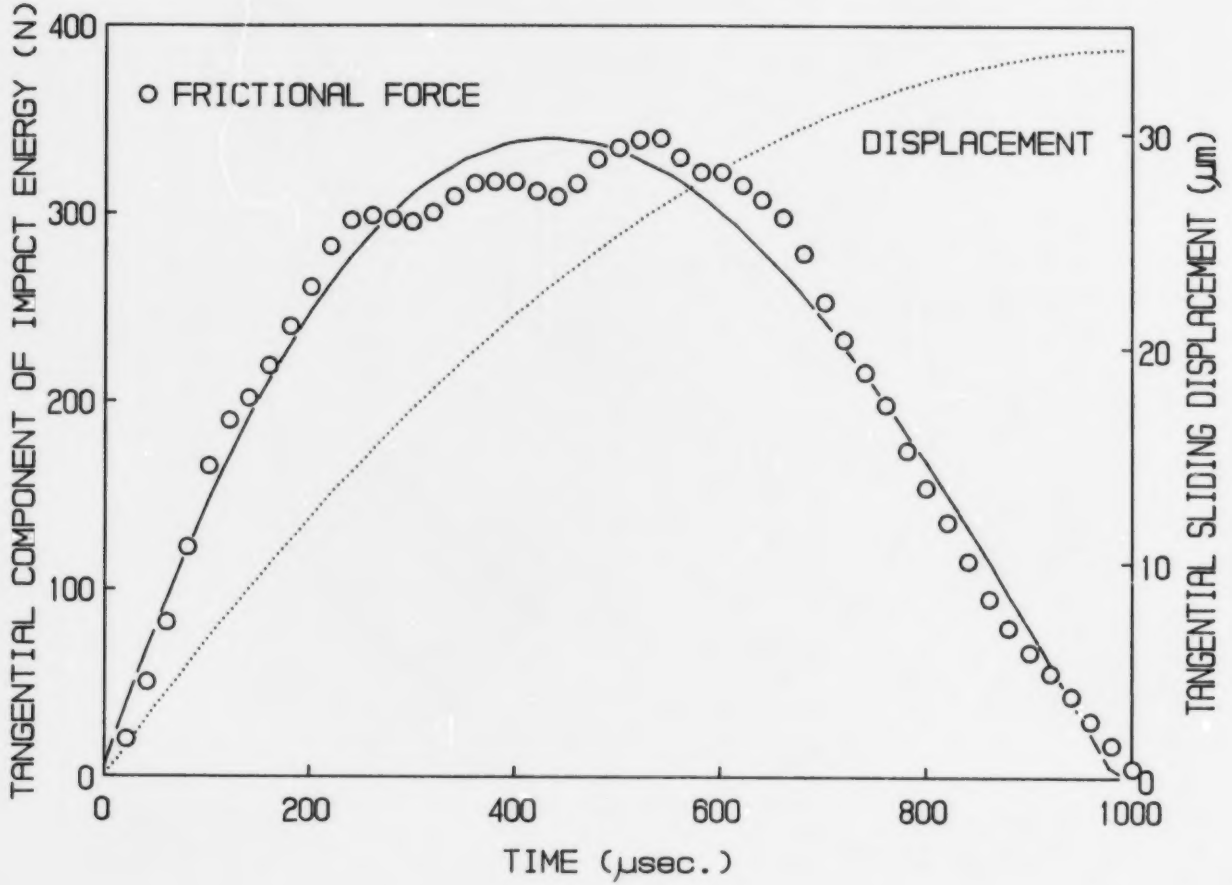


Fig. 4. Time based impact force and sliding displacement traces

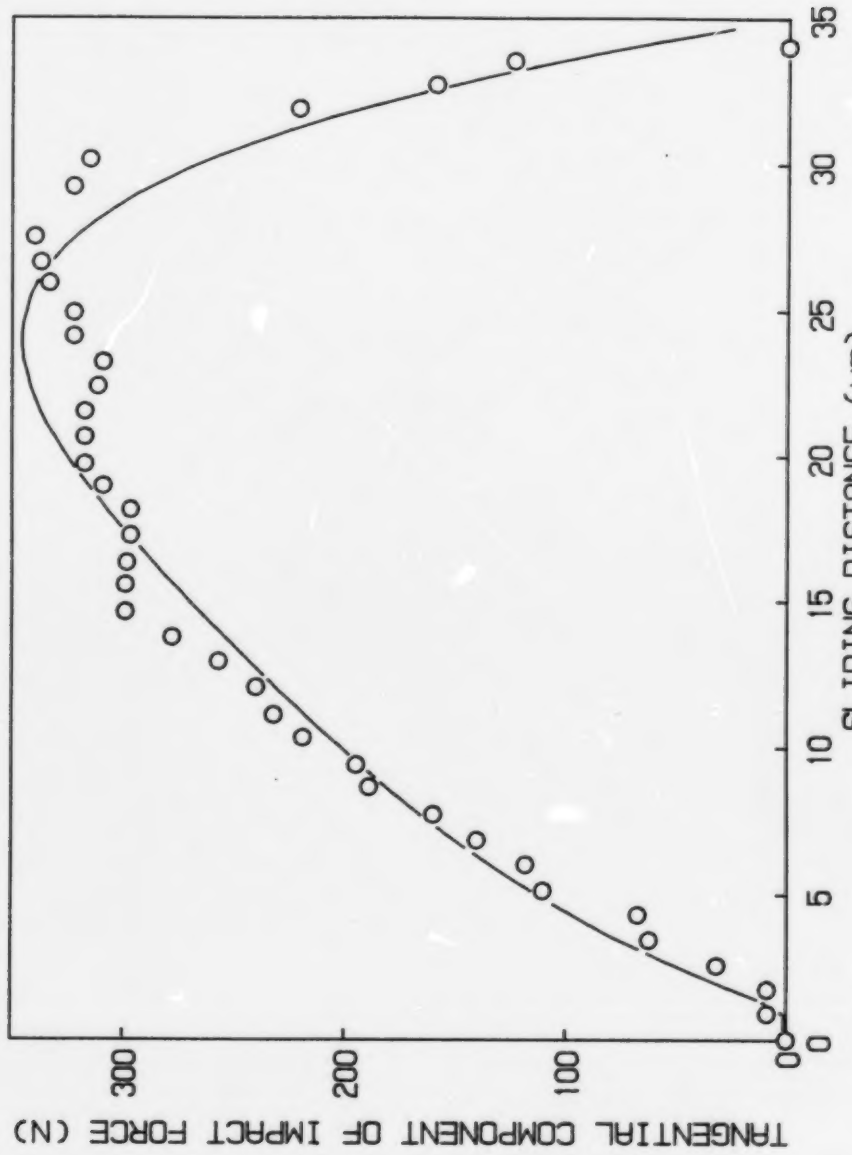


Fig. 5. Impact force vs sliding displacement

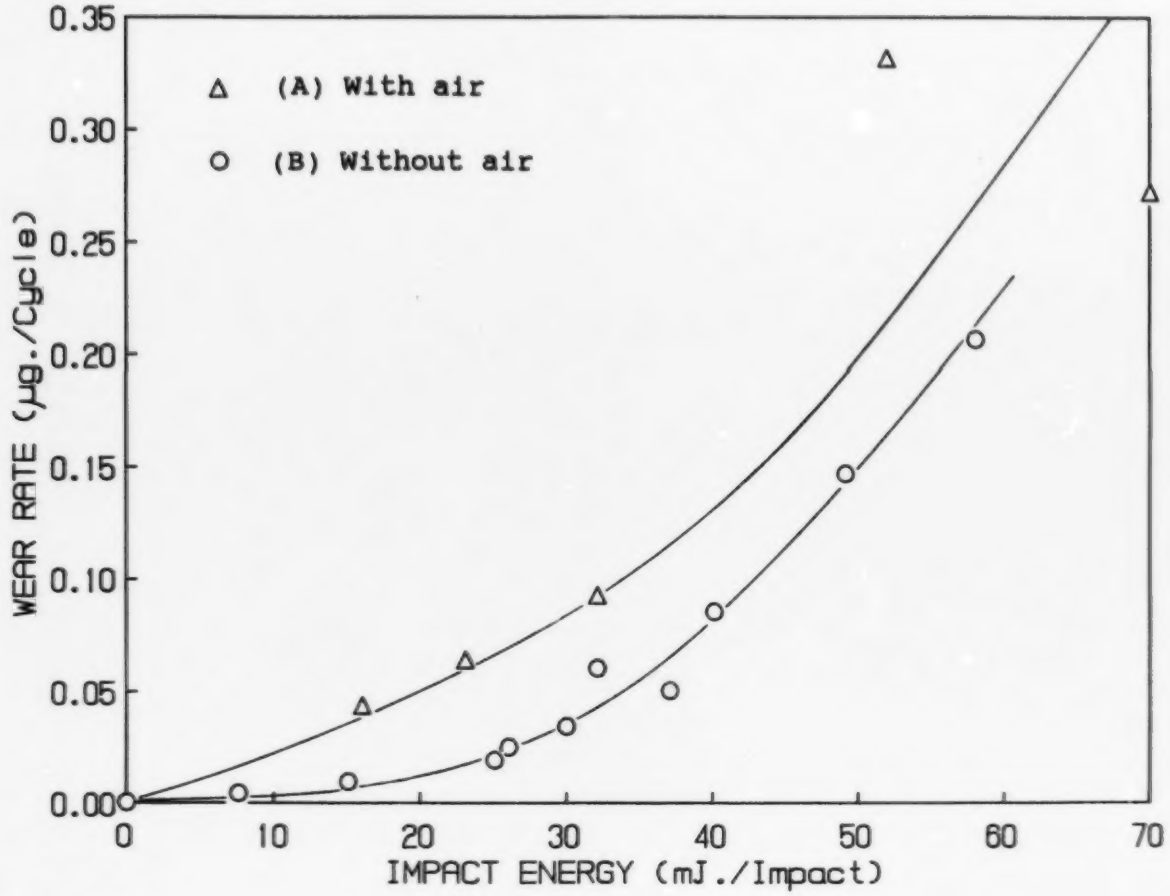


Fig. 6. Wear rate vs impact energy (steel vs steel)

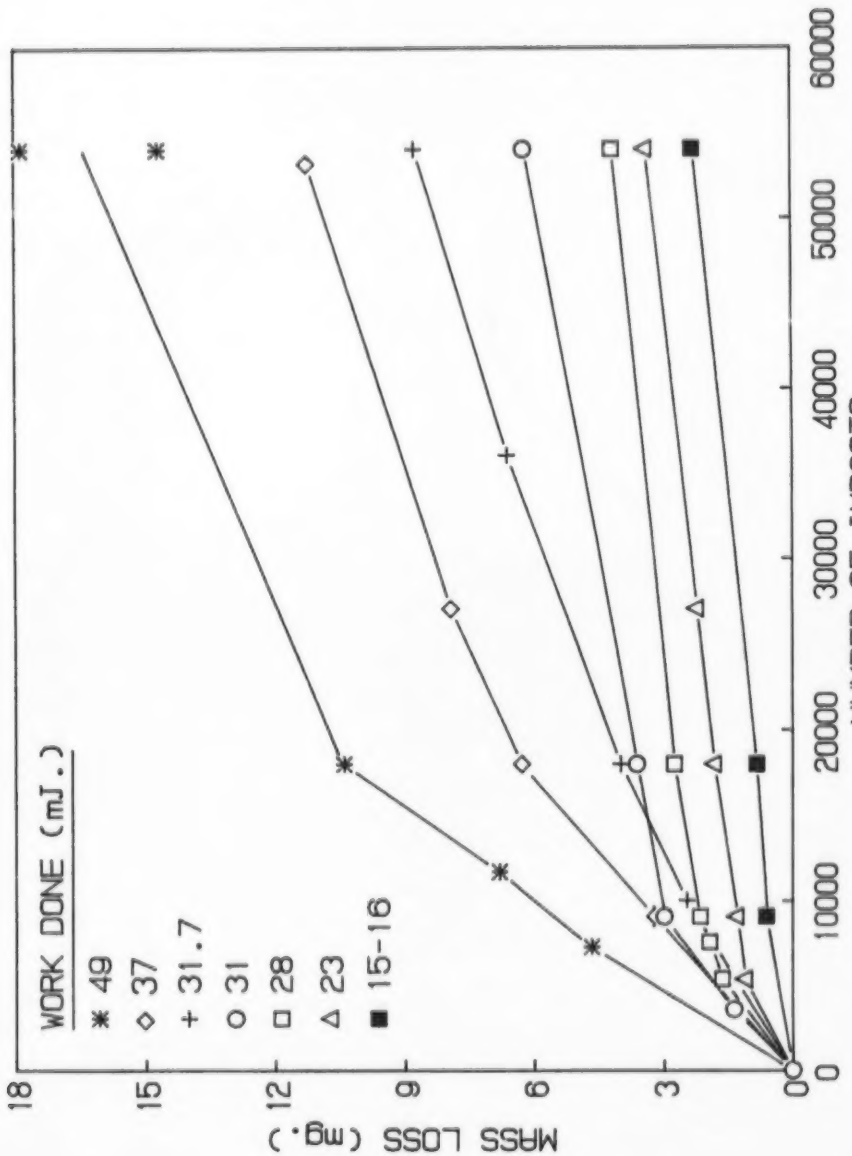


Fig. 7. Mass loss vs number of impact cycles (steel vs steel)

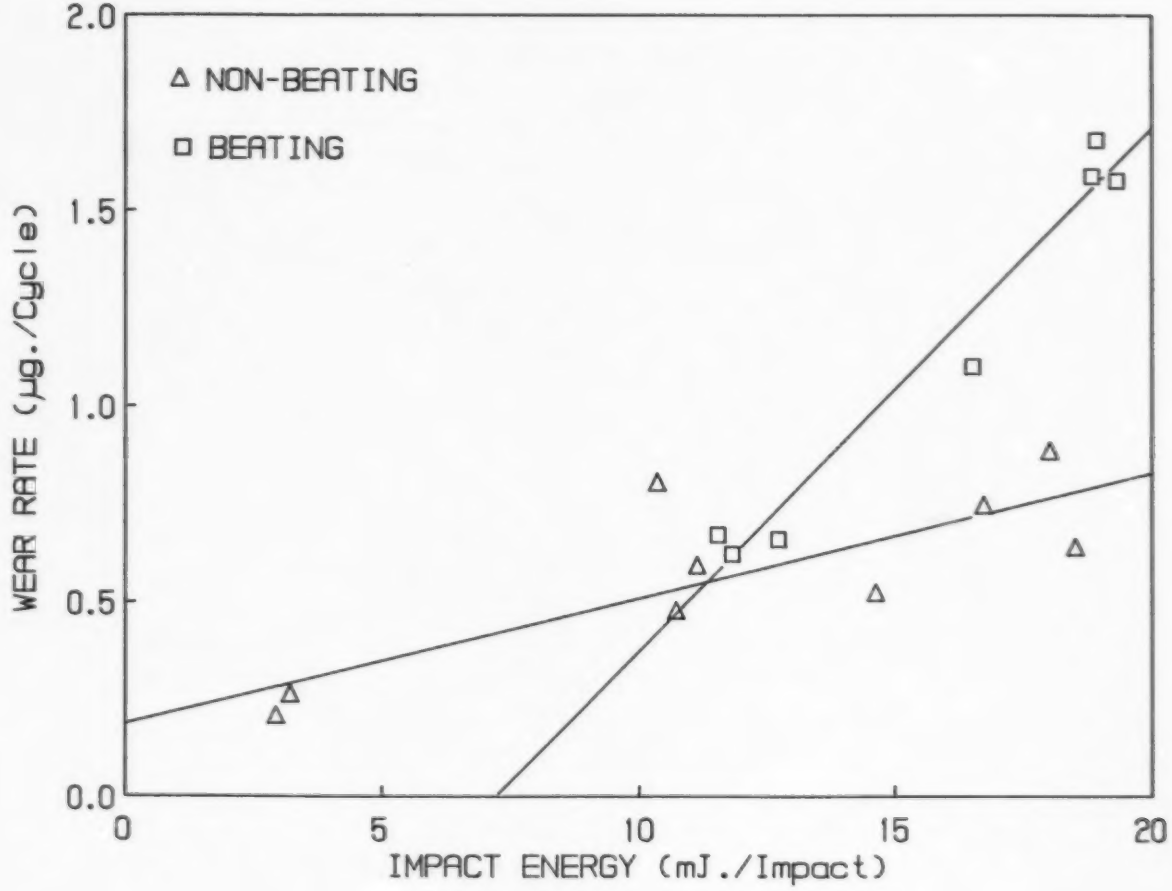


Fig. 8. Wear rate vs impact energy (steel vs brass)

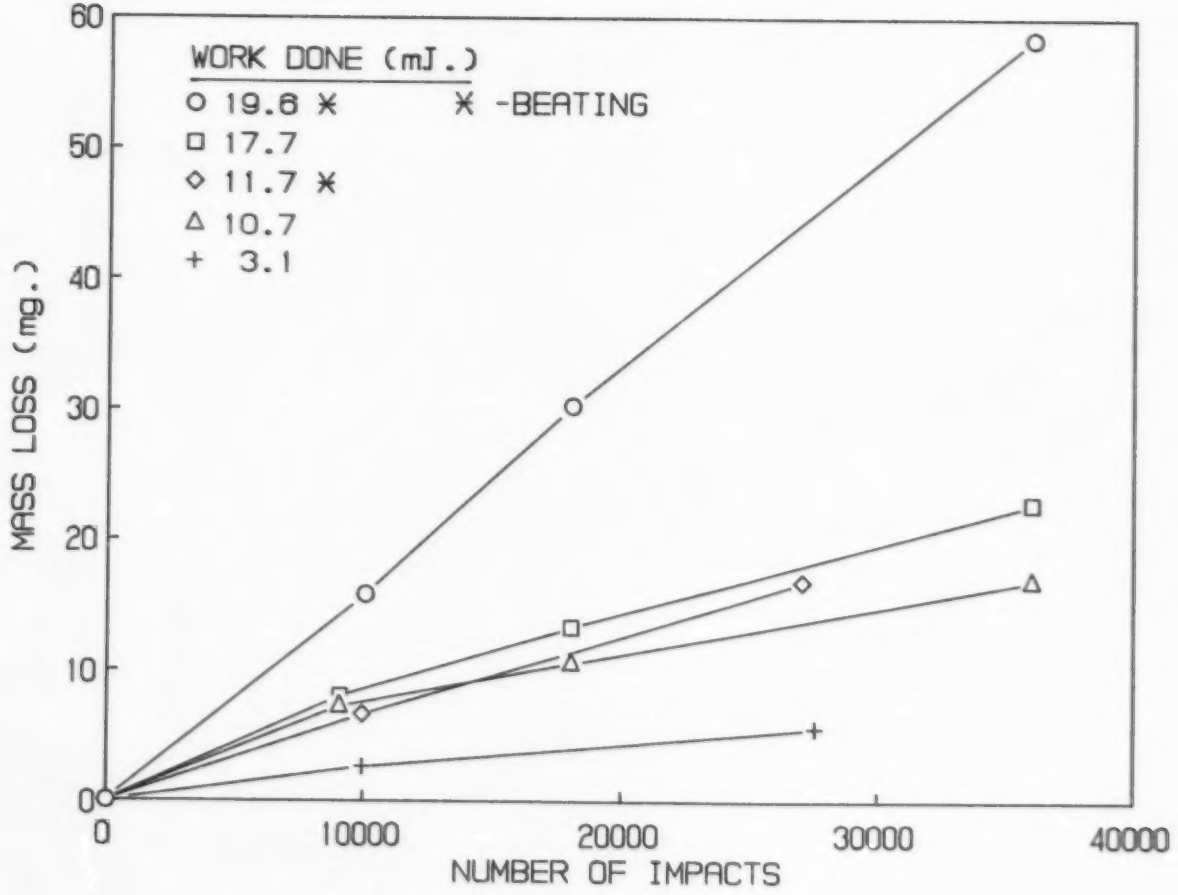


Fig. 9. Mass loss vs number of impact cycles (steel vs brass)

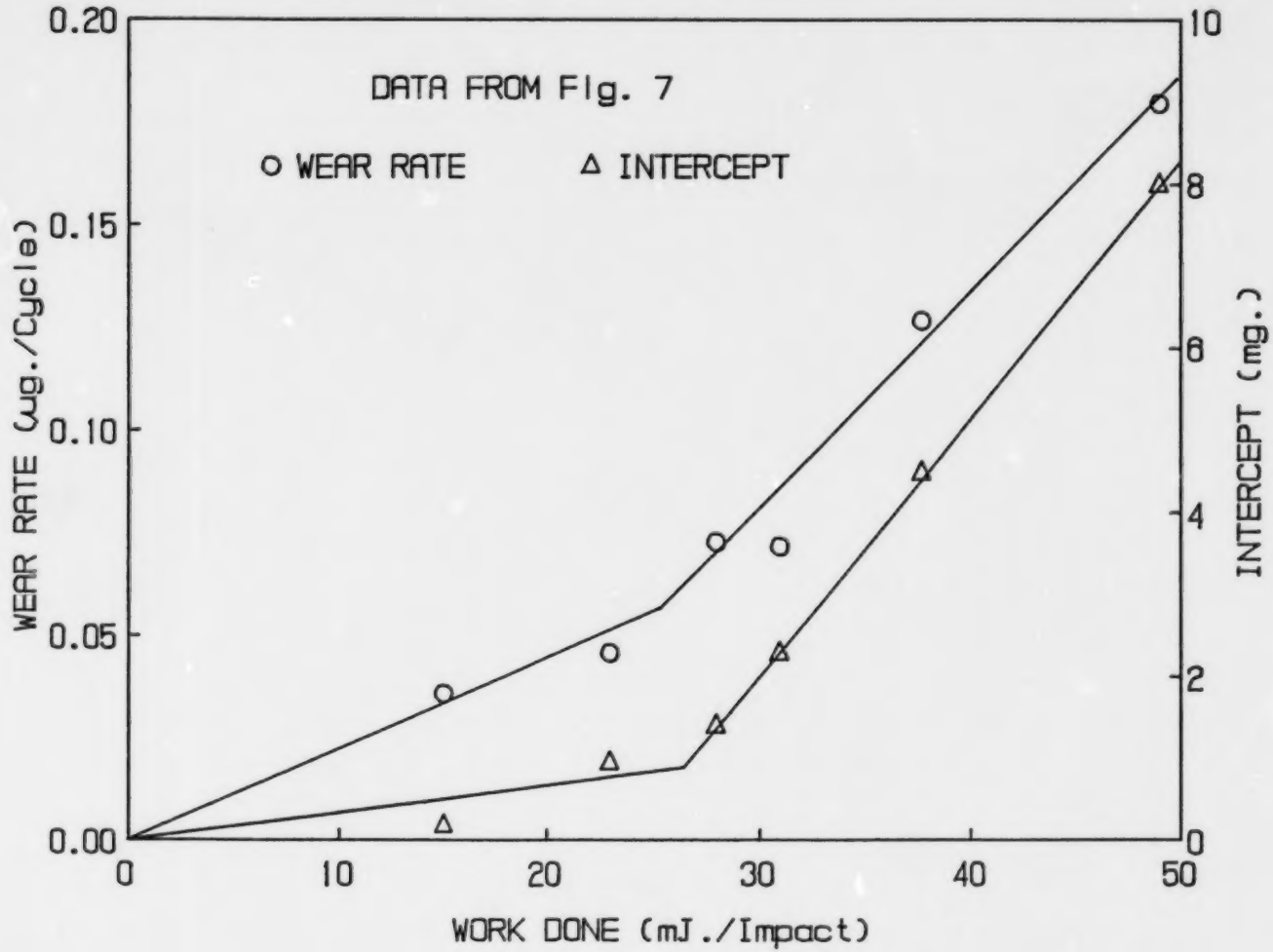


Fig. 10. Linearized wear rate vs impact energy (steel vs steel)

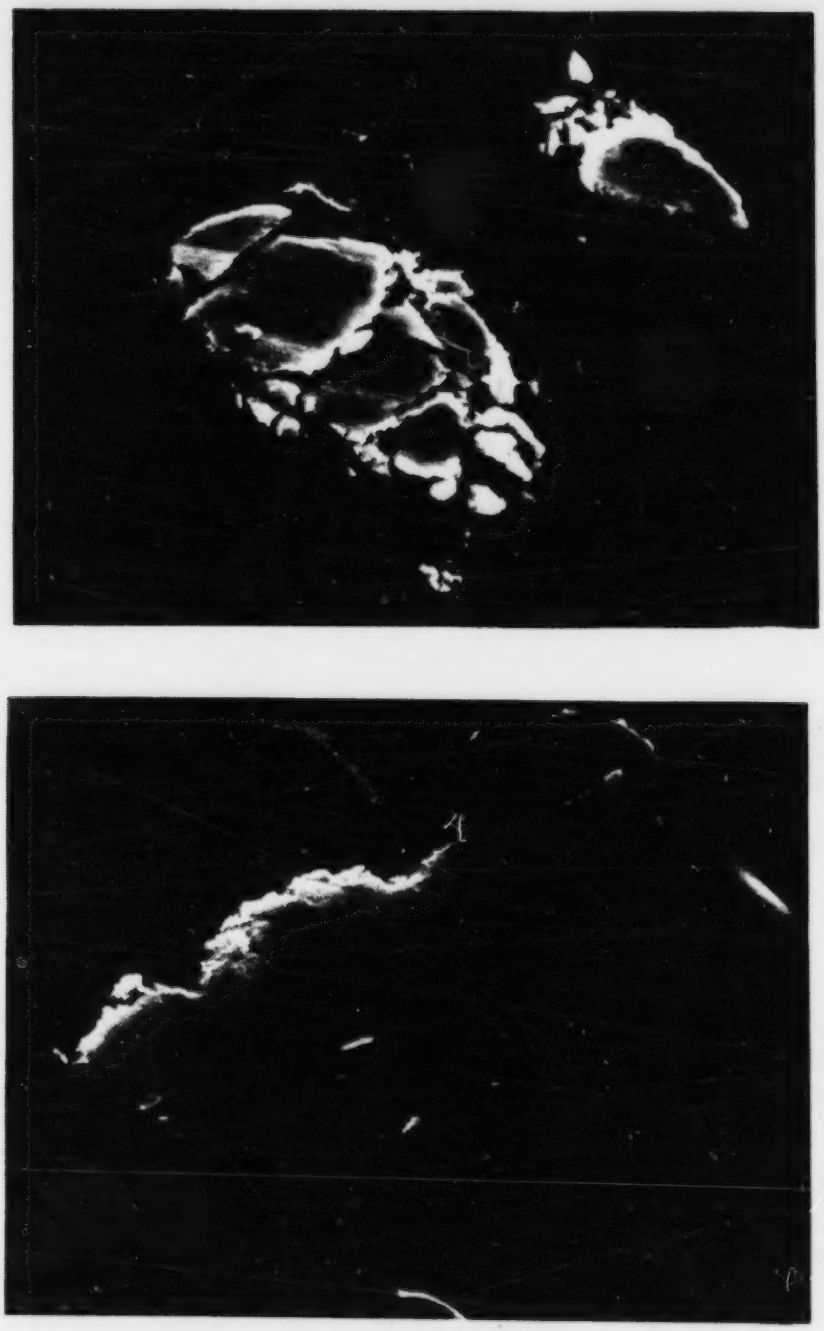

Fig. 11. Photomicrographs of steel wear particles

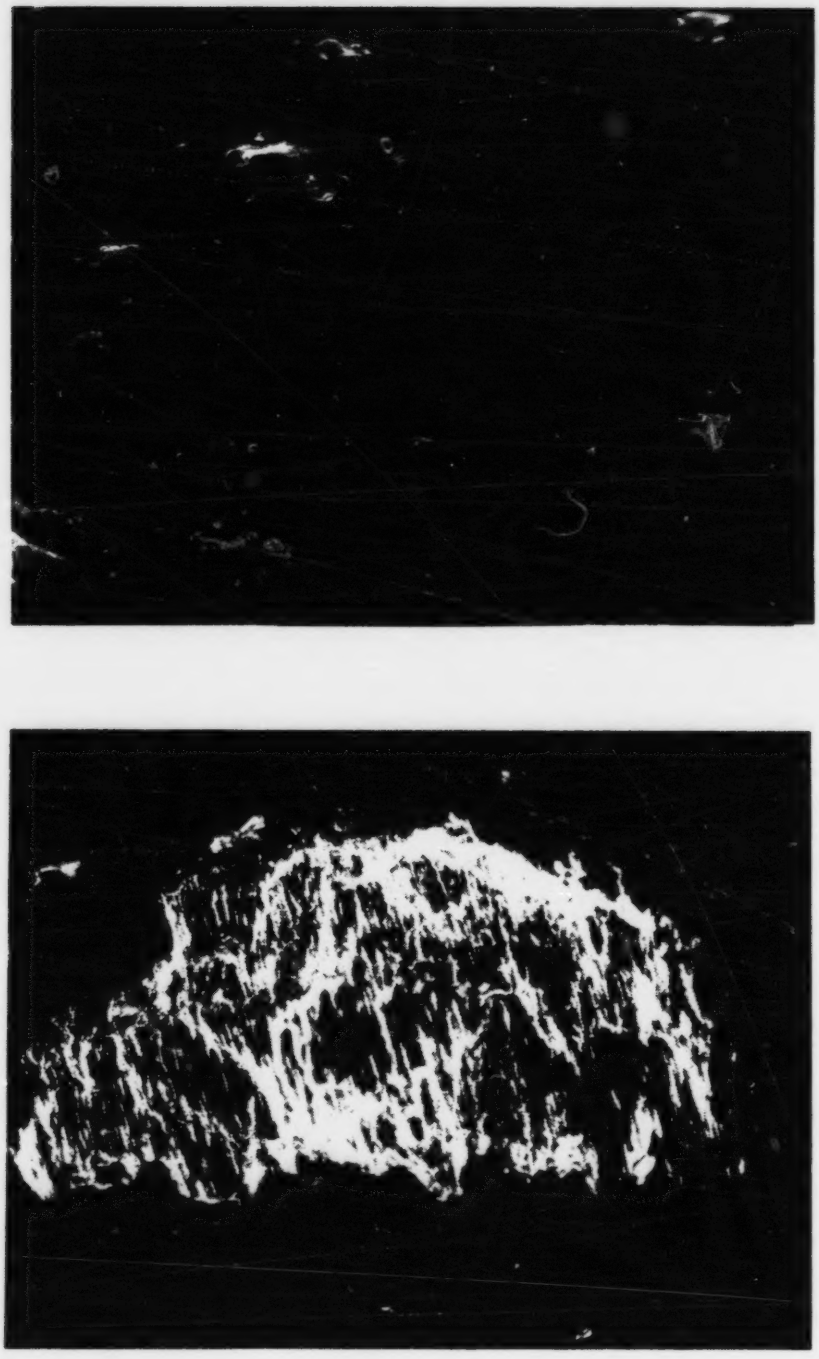

Fig. 12. Photomicrographs of brass wear particles

Fig. 13. Photographs of wear scars (steel)

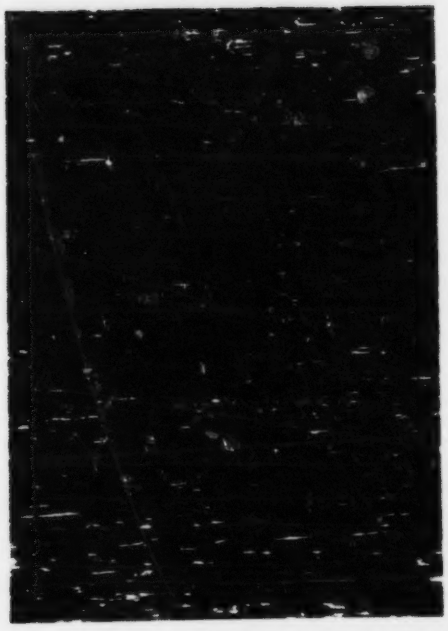

(a)

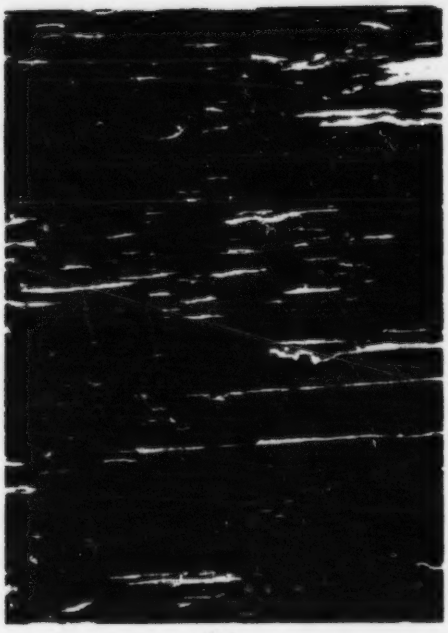

(b)

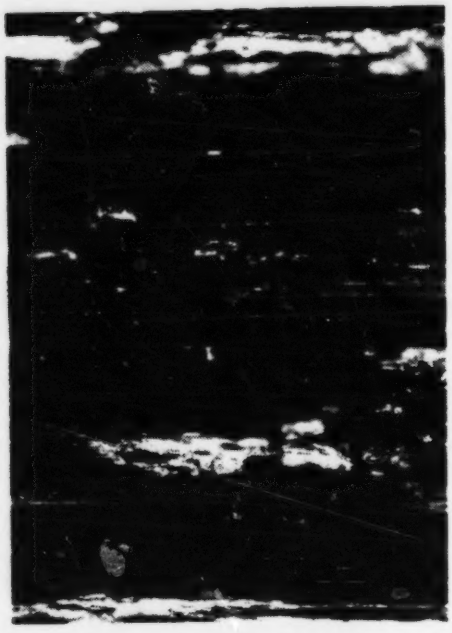

(c)

Fig. 14. Photomicrographs of wear scars
("a" steel, "b" & "c" brass)

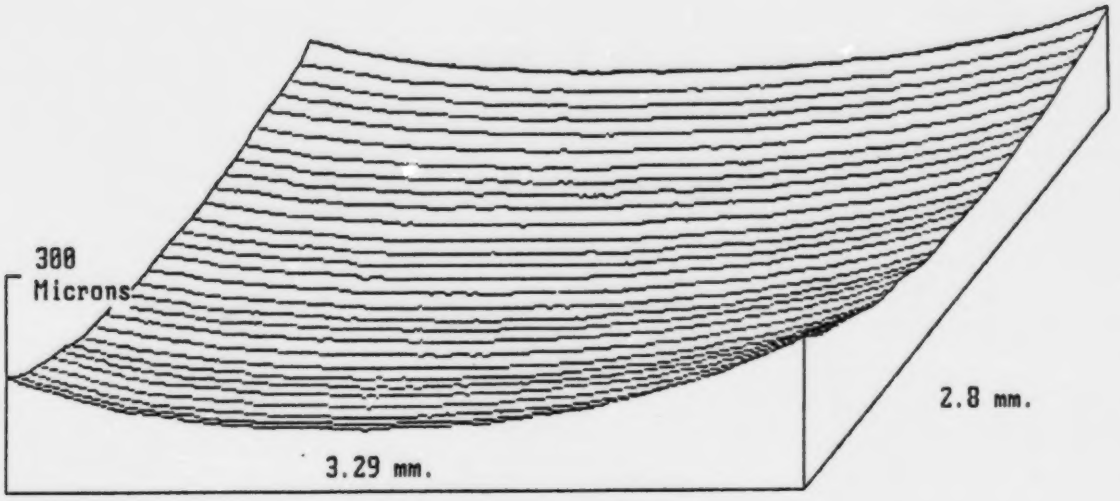


Impact hammer

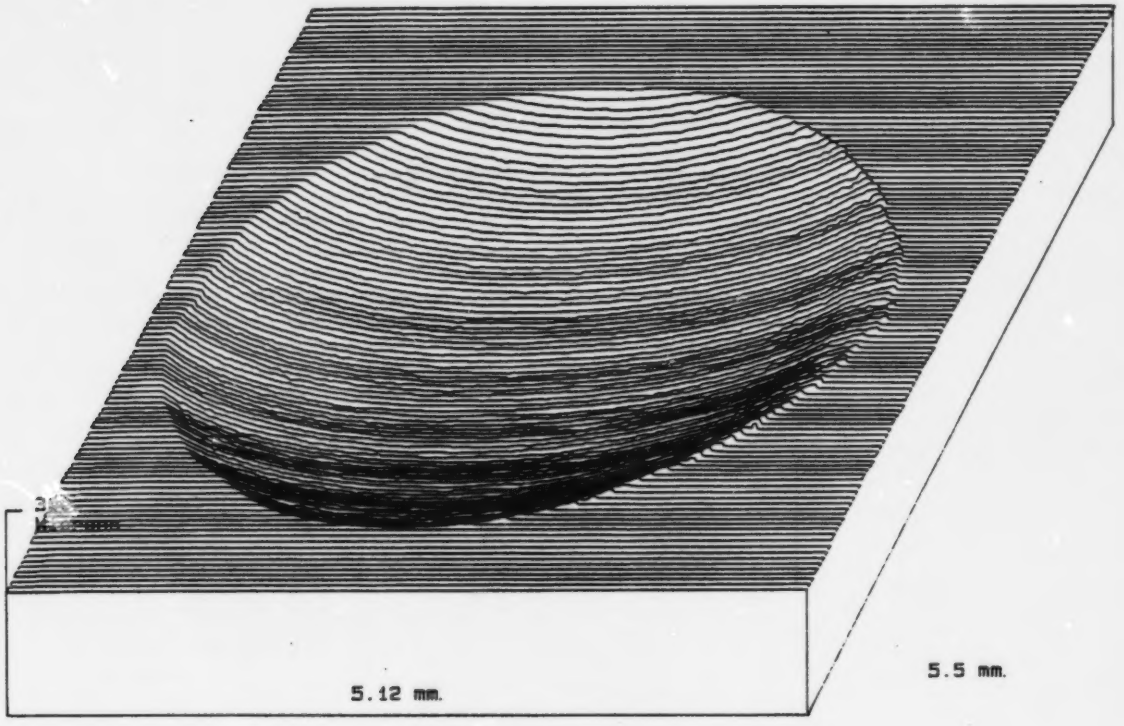


Stationary specimen

Fig. 15. Microsurface profile traces of the worn areas

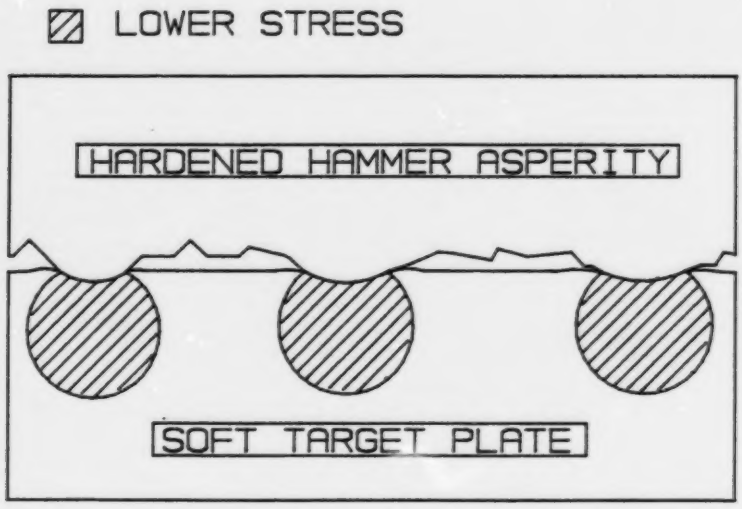


(a) Mild wear

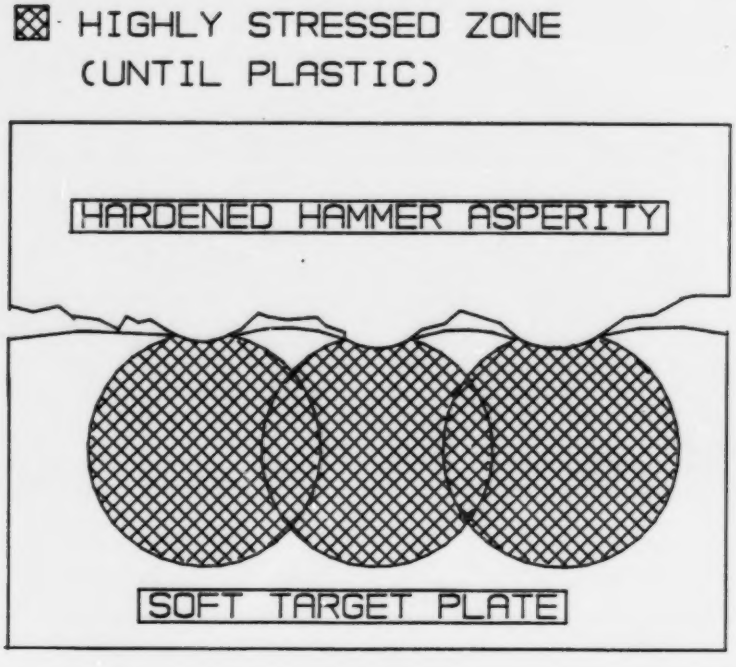


(b) Severe wear

Fig. 16. Burwell's asperity contact models

**TABLE 1 (A) MECHANICAL/PHYSICAL PROPERTIES OF SPECIMENS**

| | Carbon Steel (12L14) | Brass (C36000) | Carbon Steel (4340) |
|---|---|---|---|
| Flow pressure ($p_m$), $N.m^{-2}$ | $1.85 \times 10^9$ | $1.5 \times 10^9$ | $6.38 \times 10^9$ |
| Radius (R), m | | | 0.016 |
| Density ($\rho$), $kg.m^{-3}$ | 7860 | 8490 | 7830 |
| Yield Strength, MPa | | 124-310 | 1675 |
| Tensile Strength, MPa | | 338-469 | 1875 |
| Hardness, HB | 150 | 95 | 520-600 |

**(B) COMPOSITION RANGES AND LIMITS OF SPECIMENS**

| | C | Mn | P | S | Si | Cr | Ni | Mo |
|---|---|---|---|---|---|---|---|---|
| Carbon Steel 12L14 | 0.15 (max) | 0.85-1.15 | 0.04-0.09 | 0.26-0.35 | | | | |
| Alloy Steel 4340 | 0.38-0.43 | 0.60-0.80 | 0.035 (max) | 0.04 (max) | 0.15-0.30 | 0.70-0.90 | 1.65-2.00 | 0.20-0.30 |

| | Cu | Pb | Zn |
|---|---|---|---|
| Free Cutting Brass, C36000 | 61.5 | 3.0 | 35.5 |

**TABLE 2 TEST RESULTS AND SOME INPUT PARAMETERS OF STEEL VS STEEL**

| TEST NO | SHAKER INPUT RATIO TANG./NORM. | PEAK IMPACT FORCE (N) NORMAL | TANG. | DIST. SLID (μm) | AVG. FRICT. (N) | W.D. (mJ) | MASS LOSS (mg) | NO.OF CYCLES |
|---|---|---|---|---|---|---|---|---|
| 1 | 2.07 | 724 | 354 | 113 | 223 | 25 | 1.21 | 54000 |
| 2 | 0.87 | 762 | 367 | 32.5 | 236 | 7.6 | 0.225 | |
| 3 | 1.37 | 1121 | 594 | 85 | 349 | 30 | 1.82 | |
| 4 | 2.13 | 927.5 | 426 | 139 | 265 | 37 | 2.69 | |
| 5 | 1.56 | 950 | 415 | 96 | 270 | 26 | 1.32 | |
| 6 | 1.14 | 943 | 406 | 54 | 288 | 15 | 0.49 | |
| 7 | 1.79 | 1307 | 583 | 158 | 365 | 58 | 11.14 | |
| 8 | 0.44 | 769 | 352 | 138 | 236 | 32 | 3.22 | |
| 9 | 1.79 | 1088 | 570 | 128 | 316 | 40 | 4.61 | |
| 10 | 1.82 | 1098 | 550 | 148 | 332 | 49 | 7.91 | |
| | | The following data obtained with air jet | | | | | | |
| 11 | 0.89 | 961 | 429 | 61 | 262 | 16 | 2.30 | |
| 12 | 1.44 | 1133 | 587 | 91 | 349 | 32 | 4.96 | |
| 13 | 1.74 | 1304 | 736 | 132 | 394 | 52 | 17.84 | |
| 14 | 1.74 | 1320 | 840 | 136 | 435 | 59 | 14.66 | |
| 15 | 1.55 | 900 | 500 | 76 | 306 | 23 | 3.39 | |
| 16 | 1.77 | 944 | 466 | 105 | 290 | 31 | 1.36 | 3600 |
| 17 | 1.77 | 944 | 466 | 105 | 290 | 31 | 2.96 | 9000 |
| 18 | 1.77 | 944 | 466 | 105 | 290 | 31 | 3.61 | 18000 |
| 19 | 1.77 | 944 | 466 | 105 | 290 | 31 | 6.19 | 54000 |
| 20 | 1.46 | 809 | 439 | 67 | 232 | 15 | 0.82 | 18000 |
| 21 | 1.46 | 809 | 439 | 67 | 232 | 15 | 0.61 | 9000 |
| 22 | 1.60 | 887 | 484 | 91 | 264 | 23 | 1.8 | 18000 |
| 23 | 1.60 | 887 | 484 | 91 | 264 | 23 | 1.28 | 9000 |
| 24 | 1.60 | 887 | 484 | 91 | 264 | 23 | 2.2 | 27000 |
| 25 | 1.60 | 887 | 484 | 91 | 264 | 23 | 1.07 | 5400 |
| 26 | 1.73 | 956 | 635 | 102 | 270 | 28 | 1.91 | 7500 |
| 27 | 1.73 | 956 | 635 | 102 | 270 | 28 | 1.63 | 5400 |
| 28 | 1.73 | 956 | 635 | 102 | 270 | 28 | 2.14 | 9000 |
| 29 | 1.73 | 956 | 635 | 102 | 270 | 28 | 2.74 | 18000 |
| 30 | 1.85 | 1335 | 800 | 140 | 370 | 49 | 6.79 | 11700 |
| 31 | 1.85 | 1335 | 800 | 140 | 370 | 49 | 10.4 | 18000 |
| 32 | 1.85 | 1335 | 800 | 140 | 370 | 49 | 4.65 | 7200 |
| 33 | 1.68 | 983 | 631 | 85 | 374 | 31.7 | 6.6 | 36000 |
| 34 | 1.68 | 983 | 631 | 85 | 374 | 31.7 | 3.97 | 18000 |
| 35 | 1.68 | 983 | 631 | 85 | 374 | 31.7 | 2.43 | 10000 |
| 36 | 1.68 | 983 | 631 | 85 | 374 | 31.7 | 8.73 | 54000 |

TABLE 3 TEST RESULTS AND SOME INPUT PARAMETERS OF STEEL ON BRASS

| TEST NO. | SHAKER INPUT RATIO TANG./NORM. | PEAK IMPACT FORCE (N) NORM. | TANG. | DIST. SLID (μM) | AVE. FRICT. (N) | W.D. (mJ) | MASS LOSS (mg) | NO.OF CYCLES |
|---|---|---|---|---|---|---|---|---|
| 1 | 1.68 | 800 | 400 | 131 | 160 | 21.2 | 58.36 | 36000 |
| 2 | 1.68 | 800 | 400 | 133 | 140 | 18.8 | 15.86 | 10000 |
| 3 | 1.68 | 800 | 400 | 127 | 139 | 18.9 | 30.24 | 18000 |
| 4 | 1.00 | 876 | 386 | 55 | 197 | 11.1 | 10.59 | 18000 |
| 5 | 1.00 | 876 | 386 | 57 | 195 | 10.7 | 16.93 | 36000 |
| 6 | 1.00 | 876 | 386 | 61 | 171 | 10.3 | 7.22 | 9000 |
| 7 | 1.12 | 898 | 480 | 85 | 212 | 18 | 7.93 | 9000 |
| 8 | 1.12 | 898 | 480 | 77 | 243 | 18.5 | 22.81 | 36000 |
| 9 | 1.12 | 898 | 480 | 71 | 235 | 16.7 | 13.38 | 18000 |
| 10 | 1.60 | 624 | 285 | 91 | 131 | 11.8 | 16.77 | 27000 |
| 11 | 1.60 | 590 | 232 | 95 | 122 | 11.5 | 6.64 | 9900 |
| 12 | 0.55 | 1104 | 500 | 16 | 172 | 2.9 | 5.65 | 27500 |
| 13 | 0.55 | 1027 | 459 | 17 | 184 | 3.2 | 2.57 | 9900 |
| 14 | 1.65 | 878 | 349 | 129 | 150 | 19.3 | 56.72 | 36000 |
| 15 | 1.12 | 1015 | 521 | 83 | 199 | 16.5 | 39.44 | 36000 |
| 16 | 1.49 | 800 | 500 | 73 | 202 | 14.6 | 18.6 | 36000 |
| 17 | 0.56 | 600 | 370 | 92 | 143 | 12.7 | 25.0 | 38000 |

## REPORT DOCUMENTATION PAGE/PAGE DE DOCUMENTATION DE RAPPORT

| REPORT/RAPPORT<br>TR-TM-006<br>1a | REPORT/RAPPORT<br>NRC No. 28862<br>1b |
|---|---|
| SECURITY CLASSIFICATION/<br>CLASSIFICATION DE SÉCURITÉ<br>Unclassified<br>2 | DISTRIBUTION/DIFFUSION<br>☐ Controlled/Contrôlé<br>☒ Unlimited/Illimité<br>3 |

TITLE/SUBTITLE/TITRE/SOUS-TITRE
IMPACT AND FRETTING WEAR STUDIES
Part 2 - Room Temperature Test Results (Single Impact per Cycle)
4

AUTHOR(S)/AUTEUR(S)
Ko, P.L.; Close, L.; Robertson, M.F.
5

SERIES/SÉRIE
Technical Report
6

CORPORATE AUTHOR/PERFORMING AGENCY/AUTEUR D'ENTREPRISE/AGENCE D'EXÉCUTION
National Research Council
Division of Mechanical Engineering
Tribology and Mechanics Laboratory
7

SPONSORING AGENCY/AGENCE DE SUBVENTION
8

| DATE | FILE/DOSSIER | LAB. ORDER<br>COMMANDE DU LAB. | PAGES | DIAGS | REFS |
|---|---|---|---|---|---|
| 1988/01 | | | 27 | 19 | 13 |
| 9 | 10 | 11 | 12a | 12b | 12c |

NOTES
13

DESCRIPTORS(KEY WORDS)/MOTS-CLÉS
Tribology, wear, fretting, impact, impact-energy, fatigue
14

SUMMARY/SOMMAIRE
Impact-fretting tests were conducted in the new test rig. Results of steel vs. steel and steel vs. brass show that wear rate increases in proportional to the impact energy and that adhesive wear and fatigue are the principal mechanisms.
15

ADDRESS/ADRESSE
Dr. Clive Dayson
National Research Council
Division of Mechanical Engineering
Western Laboratories
3650 Wesbrook Mall
Vancouver, B.C. V6S 2L2 (604) 666-2623
16